*Korean J. Chem. Eng.*, 38(8), 1669-1675 (2021)
DOI: 10.1007/s11814-021-0807-3

pISSN: 0256-1115
eISSN: 1975-7220

# Optimization of preparation and properties of *Gardenia* yellow pigment-loaded alginate beads

**Yong Liu*,†, Qing Zhou*,**, Yan-Mei He*, Xiu-Yun Ma*, Lin-Na Liu*, and Yong-Jian Ke***

*School of Food and Pharmaceutical Engineering, Zhaoqing University, Zhaoqing, China
**School of Light Industry and Chemical Engineering, Guangdong University of Technology, Guangzhou, China
(*Received 7 February 2021 • Revised 24 March 2021 • Accepted 11 April 2021*)

**Abstract**−*Gardenia* yellow pigment (GYP) loaded alginate beads were prepared by the ionic gelation technique, and the preparation parameters were optimized by response surface methodology for high encapsulation efficiency. The optimized parameters were alginate concentration of 3.3%, $CaCl_2$ concentration of 2.4%, and GYP concentration of 3.2 mg/mL, under which the encapsulation efficiency was 73.61%. The surface morphology and bead size analysis showed that the GYP-loaded alginate beads had a roughly spherical morphology with a wrinkled surface, and their average diameter was 0.87 mm. In vitro release test revealed that the GYP release had a pH-dependent release profile and a two-step release process. The Rigter-Peppas model was the most proper model to assess the GYP release from alginate beads. The release mechanism of GYP at pH 1.2 and 7.4 was non-Fickian transport and case-II transport, respectively. The 2,2-diphenyl-1-picrylhydrazyl assay indicated that the encapsulated GYP had effectively maintained 82.56% of the antioxidant activity.

Keywords: Sodium Alginate, Response Surface Methodology, Release Kinetics, Antioxidant Activity, Pigment

## INTRODUCTION

In recent years, natural products from herbal plants have attracted widespread attention for their multiple biological activity and low toxicity. *Gardenia jasminoides* Ellis, an herbal plant, is widely distributed in Asia, North America, and the world's tropical and subtropical areas for its ornamental and medicinal values [1]. Its fruits are commonly used as a traditional medicine because of their biological activity, such as antioxidant, anti-inflammatory, anxiolytic, anti-hypertension, antidepressant, antidiabetic, hypoglycemic, and neuroprotective [2-5]. *Gardenia* yellow pigment (GYP) from the fruits is a water-soluble carotenoid mainly comprised of crocetin and crocin [6]. The Chinese and Japanese governments have approved it for use as a food additive [7]. At present, GYP has been used in foods to color candy, pastries, noodles, and beverages for its excellent water solubility and health benefits [1,8]. It is widely known that natural pigments are vulnerable to adverse environmental conditions, such as pH variation, water activity, high temperature, light exposure, metal ions, oxygen, and enzymes, leading to a reduction in their stability and biological activity [9-11]. Therefore, it is essential to apply effective technology to protect natural pigments for their application and long-term storage.

Microencapsulation technology, widely used in the food industry, is an effective technique to protect food bioactive ingredients against deterioration due to its low cost and flexibility [9,12]. Moreover, it can isolate the bioactive ingredients from the external environment, maintain their original performance and activity, control their release rate, and extend their storage time [13-15]. Ionic gelation is a widely used microencapsulation technique for food products due to its practicality, versatility, simplicity, efficiency, and low-cost [16]. This technique is based on the cross-linking of polyelectrolyte chains in the presence of multivalent cations to encapsulate and protect bioactive ingredients [17]. Sodium alginate (SA) is a natural anionic polysaccharide with carboxyl end groups. It has been widely employed as a wall material to encapsulate bioactive compounds based on its carboxyl groups' cross-linking and multivalent cations such as calcium ions [11,17-20]. Because of its ionic gelation properties, the alginate-based beads have been successfully fabricated to encapsulate and protect some bioactive compounds such as *Bougainvillea spectabilis* extracts [21], oregano essential oil [22], cumin seeds essential oil [23], beetroot betacyanins and polyphenols [24], natural astaxanthin [25], and jussara anthocyanins [26].

This work prepared GYP-loaded alginate beads by ionic gelation technique and optimized preparation parameters by response surface methodology (RSM). The proposed beads were characterized for encapsulation efficiency, bead size distribution, morphology, antioxidant activity, and release kinetics.

## EXPERIMENTAL

### 1. Materials and Chemicals

Desiccative ripe *Gardenia* fruits were provided by a farm in Huaiji County, Zhaoqing City. Sodium alginate (SA), 2,2-diphenyl-1-picrylhydrazyl (DPPH), and vitamin C were purchased from Macklin Biochemical Technology Co. Ltd. (Shanghai, China).

### 2. Extraction of GYP

GYP was extracted from desiccative ripe *Gardenia* fruits accord-

†To whom correspondence should be addressed.
E-mail: lygdut@163.com

**Table 1. Box-Behnken design for preparation parameters and encapsulation efficiency**

| Run | Coded values (uncoded values) of preparation parameters | | | Y (%) |
|---|---|---|---|---|
| | A (%) | B (%) | C (mg/mL) | |
| 1 | 2.5 (−1) | 3.0 (1) | 3.0 (0) | 55.01 |
| 2 | 2.5 (−1) | 2.5 (0) | 4.0 (1) | 60.12 |
| 3 | 3.5 (1) | 2.5 (0) | 4.0 (1) | 67.58 |
| 4 | 3.0 (0) | 2.0 (−1) | 4.0 (1) | 68.86 |
| 5 | 2.5 (−1) | 2.5 (0) | 2.0 (−1) | 57.22 |
| 6 | 3.0 (0) | 2.5 (0) | 3.0 (0) | 71.79 |
| 7 | 3.0 (0) | 3.0 (1) | 2.0 (−1) | 55.04 |
| 8 | 3.5 (1) | 2.5 (0) | 2.0 (−1) | 65.79 |
| 9 | 3.0 (0) | 2.5 (0) | 3.0 (0) | 71.45 |
| 10 | 2.5 (−1) | 2.0 (−1) | 3.0 (0) | 62.18 |
| 11 | 3.0 (0) | 3.0 (1) | 4.0 (1) | 58.18 |
| 12 | 3.5 (1) | 3.0 (1) | 3.0 (0) | 66.82 |
| 13 | 3.5 (1) | 2.0 (−1) | 3.0 (0) | 68.36 |
| 14 | 3.0 (0) | 2.5 (0) | 3.0 (0) | 72.54 |
| 15 | 3.0 (0) | 2.0 (−1) | 2.0 (−1) | 60.17 |

ing to our previous work [27] with a slight modification. The dried fruits were crushed by a laboratory mill and passed through an 80-mesh sieve to obtain fruit powder. The powder (2.0 g) was dispersed in a flask containing 160 mL of 50% ethanol solution, and then the flask was placed in an ultrasonic generator to extract for 40 minutes. The extraction solution was centrifuged at 10,000 rpm for 20 min and then concentrated by a vacuum rotary evaporator. Finally, the concentrated solution was freeze-dried to obtain GYP and stored in a desiccator for later use.

**3. Preparation of GYP-loaded Alginate Beads and Determination of Encapsulation Efficiency**

GYP-loaded alginate beads were prepared by ionic gelation technique. Briefly, SA and GYP were dissolved in distilled water to make a uniform mixed solution. The mixture was dripped at room temperature at a rate of 60 drops/min with a 13-gauge needle syringe into a $CaCl_2$ solution stirred at 200 rpm. After that, the beads were soaked in the $CaCl_2$ solution for 5 min. Finally, the beads were recovered by filtration and washed with 30 mL distilled water, after which the beads were freeze-dried for 48 h at −40 °C and a vacuum of 20 Pa and stored in a desiccator until their use. The filtrate and washing liquid were collected in a volumetric flask, in which the absorbance was determined at 440 nm by a UV-vis spectrophotometer [28], and the free GYP weight was obtained using the established GYP standard curve. The encapsulation efficiency (EE) of GYP in the beads was calculated by Eq. (1):

$$\text{EE}\ (\%) = \frac{\text{total GYP weight} - \text{free GYP weight}}{\text{total GYP weight}} \times 100\% \quad (1)$$

**4. Optimization of Preparation Parameters for GYP-loaded Alginate Beads**

According to the pre-test, the preparation parameters like alginate concentration (A), $CaCl_2$ concentration (B), and GYP concentration (C) for the GYP-loaded alginate beads were optimized by Box-Behnken design with encapsulation efficiency (Y) used as the optimization index. Design-Expert software (version 8.06) was used to perform 15 runs with three center points. The parameter levels and tests are given in Table 1.

**5. Measurement of Surface Morphology and Bead Size**

The surface morphology of the GYP-loaded alginate beads was measured by SEM (Supra55, Zeiss, Germany), and their size distribution was investigated by a digital micrometer (CN63M, Yuanhengtong, China). One hundred beads were randomly selected to determine their diameter. Each bead was measured four times in its different positions and its size was taken as the average value.

**6. Antioxidant Activity of GYP**

The antioxidant activity of GYP was evaluated by DPPH assay [29] using ascorbic acid (Vc) as a standard. Its antioxidant activity was expressed as Vc milliequivalents per milligram of GYP (mg Vc/mg).

**7. Release Kinetics of GYP**

The GYP-loaded alginate beads were placed into a dialysis bag and sealed. The dialysis bag was put in an Erlenmeyer flask containing 30 mL of buffer and then was placed in an oscillator to release GYP at 37 °C at an oscillatory speed of 60 rpm. At intervals, 2 mL buffer was taken out from the flask to measure the GYP concentration according to its standard curve, and then 2 mL buffer was immediately replenished back to the flask to maintain a constant release volume solution. The cumulative release fraction of GYP was calculated by Eq. (2):

$$Q_t = \frac{M_t}{M_\infty} \quad (2)$$

where $Q_t$ is the cumulative release fraction of GYP at the time t, %; $M_t$ and $M_\infty$ represent the amount of GYP released at time t and equilibrium, respectively, μg.

According to the release data, the release kinetics and release mechanism of GYP from the beads were analyzed by four commonly-used kinetics models such as zero-order (Eq. (3)), first-order (Eq. (4)), Higuchi (Eq. (5)), and Rigter-Peppas (Eq. (6)) models [30]. The models were as follows:

$$Q_t = \frac{M_t}{M_\infty} = kt \quad (3)$$

$$Q_t = \frac{M_t}{M_\infty} = 1 - e^{-kt} \quad (4)$$

$$Q_t = \frac{M_t}{M_\infty} = kt^{1/2} \quad (5)$$

$$Q_t = \frac{M_t}{M_\infty} = kt^{n} \quad (6)$$

where k is the release constant, and n represents the release kinetic exponent indicating the GYP release mechanism.

To further explore whether the diffusion or the matrix's swelling was dominant in the non-Fickian and case-II transport, the following Peppas-Sahlin equation [31] was applied to analyze the predominant mechanism.

$$Q_t = \frac{M_t}{M_\infty} = k_1 t^{m} + k_2 t^{2m} \quad (7)$$

where $k_1$ and $k_2$ represent the Fickian diffusion and matrix's swelling constant, respectively; m is the diffusion exponent and equals 0.43 for a sphere.

## RESULTS AND DISCUSSION

### 1. Optimization of Preparation Parameters

1-1. Mathematical Model Fitting and Analysis of Variance

According to the data in Table 1, the model fitting was carried out by Design-Expert software with encapsulation efficiency (Y) as the response and alginate concentration (A), $CaCl_2$ concentration (B), and GYP concentration (C) as the independent variables. The fitted model was shown below:

$$Y = 71.93 + 4.25A - 3.07B + 2.06C + 1.41AB - 0.28AC - 1.39BC - 3.36A^2 - 5.47B^2 - 5.89C^2$$

Analysis of variance for the model in Table 2 revealed that $R^2$ and $R^2_{adj}$ were 0.9740 and 0.9272, respectively, showing that the model was reasonable to predict the test data. The model's *p*-value was 0.0019<0.05, which demonstrated the model for the encapsulation efficiency was statistically significant. The *p*-value of the lack of fit was 0.0670>0.05, meaning the model helped interpret the experimental result. The high adequate precision (12.96>4) and the low coefficients of variation (C.V. %=2.59) suggested the adequate signal and reliability of the performed tests. According to the *p*-values, the influences of linear coefficients (A, B, and C) and quadratic term coefficients ($A^2$, $B^2$, and $C^2$) on the encapsulation efficiency (Y) were significant for $p<0.05$, showing the influences on the encapsulation efficiency (Y) were non-linear. In contrast, interaction term coefficients (AB, AC, and BC) were not significant for $p>0.05$, indicating the effects of interaction between the three parameters on the encapsulation efficiency (Y) were not significant. The significant effect of the three parameters (A, B, and C) on the encapsulation efficiency (Y) was in the order of alginate concentration (A), $CaCl_2$ concentration (B), and GYP concentration (C), which showed the alginate concentration had the greatest impact on the encapsulation efficiency but the GYP concentration had the least impact.

1-2. Response Surface Analysis

The response surface and contour plots and perturbation graph of alginate concentration (A), $CaCl_2$ concentration (B), and GYP concentration (C) on the encapsulation efficiency (Y) are depicted in Fig. 1. As observed in Fig. 1(a)-(c), each response surface had the highest point, and the highest point's 2D contours were in the range of the chose parameter levels, revealing that the parameter levels for the optimization preparation of GYP-loaded alginate beads were suitable. Moreover, the 2D contours were almost circular, which showed the interactions of alginate concentration (A) and $CaCl_2$ concentration (B), alginate concentration (A) and GYP concentration (C), and $CaCl_2$ concentration (B) and GYP concentration (C) insignificantly affected the encapsulation efficiency (Y). This result agreed with the analysis of variance in Table 2.

As shown in Fig. 1(a)-(d), the encapsulation efficiency (Y) in-

**Table 2. ANOVA for the fitted quadratic model**

| Source | Sum of squares | Degree of freedom | Mean square | *F*-value | *p*-Value |
|---|---|---|---|---|---|
| Model | 515.84 | 9 | 57.32 | 20.80 | 0.0019 |
| A | 144.67 | 1 | 144.67 | 52.51 | 0.0008 |
| B | 75.15 | 1 | 75.15 | 27.28 | 0.0034 |
| C | 34.11 | 1 | 34.11 | 12.38 | 0.0169 |
| AB | 7.92 | 1 | 7.92 | 2.88 | 0.1507 |
| AC | 0.31 | 1 | 0.31 | 0.11 | 0.7517 |
| BC | 7.70 | 1 | 7.70 | 2.79 | 0.1554 |
| $A^2$ | 41.67 | 1 | 41.67 | 15.13 | 0.0115 |
| $B^2$ | 110.66 | 1 | 110.66 | 40.17 | 0.0014 |
| $C^2$ | 128.08 | 1 | 128.08 | 46.49 | 0.0010 |
| Residual | 13.78 | 5 | 2.76 | | |
| Lack of fit | 13.15 | 3 | 4.38 | 14.10 | 0.0670 |
| Pure error | 0.62 | 2 | 0.31 | | |
| Cor. total | 529.62 | 14 | | | |
| $R^2$=0.9740 | $R^2_{adj}$=0.9272 | | | | |

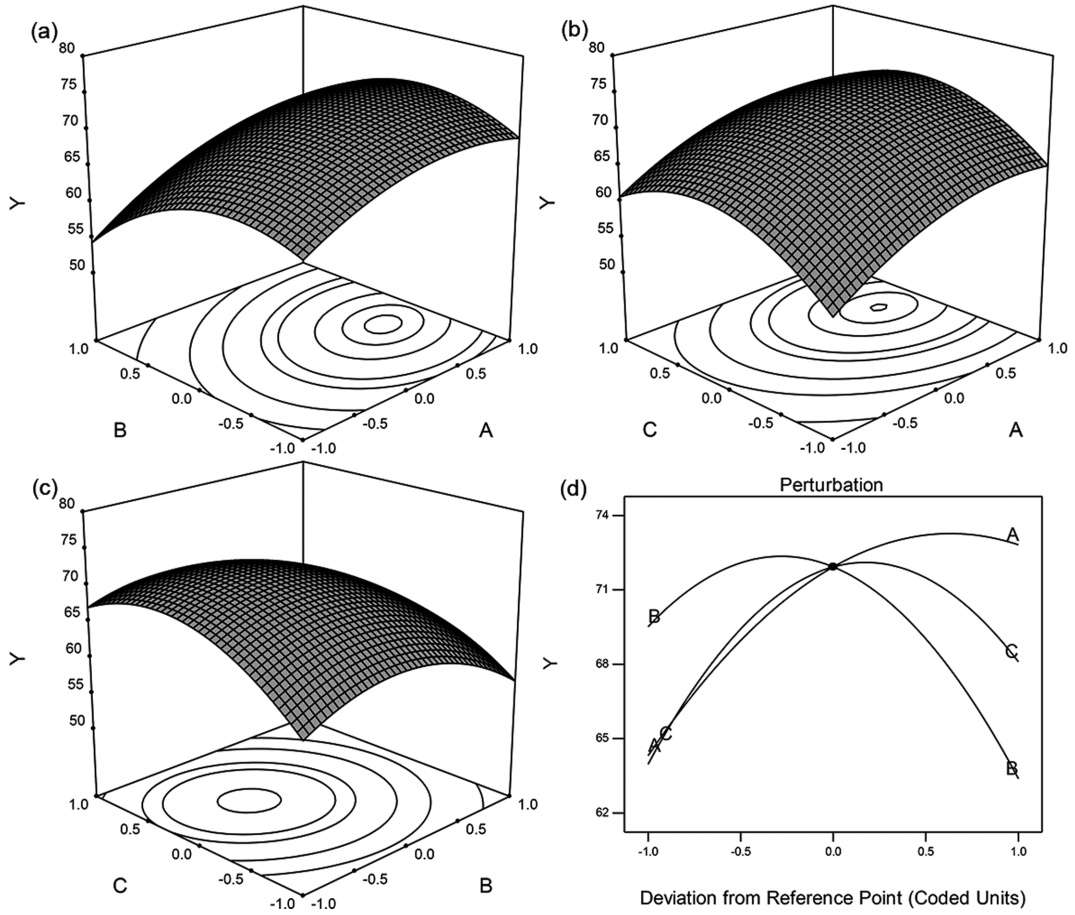


**Fig. 1. Response surface and contour plots and perturbation graph of alginate concentration (A), $CaCl_2$ concentration (B), and GYP concentration (C) on the encapsulation efficiency (Y).**

creased first and then decreased with the increment of alginate concentration (A), $CaCl_2$ concentration (B), and GYP concentration (C). It was reported that the encapsulation efficiency was associated with the microstructure and pore size of alginate matrices [32-34]. The increment of alginate concentration increased the free volume and pore size in the beads and improved the beads' tightly cross-linked network structure to retard the entrapped GYP leakage [25,35], which increased the encapsulation efficiency. However, when the alginate concentration continued to increase, the space in the beads occupied by alginate increased, resulting in the denser structure with less porous structure and smaller pore size, which reduced the encapsulation efficiency [23,25]. A similar result was found in the encapsulation of immunoglobulin Y [36]. Besides, with the increment of $CaCl_2$ concentration, the crosslinking degree of beads increased and therefore slowed the leakage of GYP from the beads [25,37], leading to the high encapsulation efficiency. However, the higher $CaCl_2$ concentration caused lower encapsulation efficiency due to the electrostatic repulsion and attraction with calcium and chlorine ions, respectively, which increased the GYP leakage from the beads [38]. Jing reported that the encapsulation efficiency of $\beta$-glucuronidase increased with the increment of $CaCl_2$ concentration to a certain level, and then reduced at higher $CaCl_2$ concentration [39]. Similar results were also shown in the encapsulation of immunoglobulin Y [36], cinnamon essential oils [40], and tea tree oil [41]. Additionally, the GYP concentration showed a quadratic effect on the encapsulation efficiency, which was related to the critical concentration of GYP in the beads [42], that is, the free volume and pore size of alginate in the mixture was sufficient to encapsulate GYP below the critical concentration, but not enough to encapsulate GYP beyond the critical concentration. This finding was also consistent with the encapsulation of immunoglobulin Y [36], cinnamon essential oils [40], and tea tree oil [41].

1-3. Predictive Model Verification

The fitting model's optimum parameters for preparing the GYP-loaded alginate beads were calculated and slightly modified for practical operation convenience. They were alginate concentration of 3.3%, $CaCl_2$ concentration of 2.4%, and GYP concentration of 3.2 mg/mL. Under these conditions, the encapsulation efficiency was 73.61%, which was 0.15% different from the predicted value, indicating the model was reasonable.

**2. Morphology and Bead Size Analysis**

The surface morphology and bead size distribution of the lyophilized GYP-loaded alginate beads prepared using the optimal parameters are shown in Fig. 2. Fig. 2(a) reveals that the beads exhibited a roughly spherical morphology with a wrinkled surface. The spherical shape was ascribed to the tighter network structure

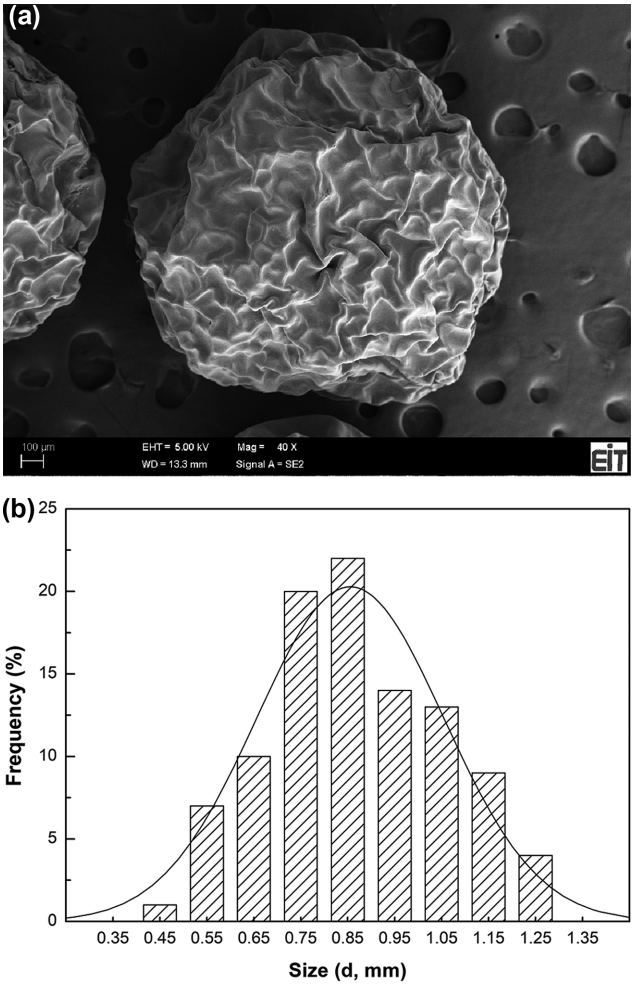


**Fig. 2. Surface morphology (a) and bead size distribution (b) of GYP-loaded alginate beads.**

and higher mechanical stability of the beads due to the rapid cross-linking and high alginate concentration [43]. Simultaneously, the wrinkled surface was attributed to the water evaporated from the bead's pore paths during dehydration, resulting in bead shrinkage [44]. Arriola [16], Busic [45], and Belscak-Cvitanovic [46] also reported similar observations. The bead size distribution of the GYP-loaded alginate beads was statistically analyzed according to the measured data, and the results shown in Fig. 2(b). The bead size had a normal distribution with an average diameter of 0.87 mm. The highest frequency was 22% at 0.85 mm, which confirmed the bead size normal distribution and average diameter. Similar size distribution was also observed in the anthocyanins-loaded alginate-based beads [26].

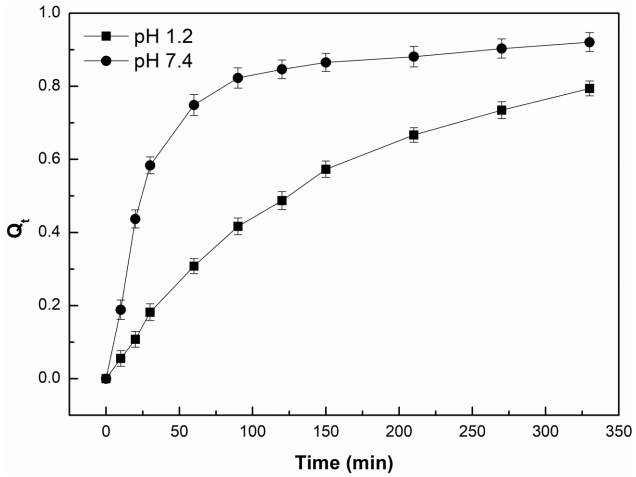


**Fig. 3. Release profiles of GYP from alginate beads at pH 1.2 and 7.4.**

### 3. Release Kinetics and Antioxidant Activity Analysis

In vitro release profiles of GYP from the optimized alginate beads at 37°C in a simulated gastric buffer (pH 1.2) and a simulated intestinal buffer (pH 7.4) are presented in Fig. 3. A two-step release process, which began with a rapid release and subsequently a slow-release, was observed. The initial rapid release process was attributed to the presence of GYP on the bead surface and the easy release of the hydrophilic GYP from the bead's porous structure [47]; while the slow-release process was due to the release of GYP from the bead core and the decrease of GYP concentration difference inside and outside the beads. A similar result was also found in the tea polyphenol release from the alginate-based beads [44].

As shown in Fig. 3, a pH-dependent release pattern of GYP was also found. Thus, the GYP release was lower at pH 1.2 but higher at pH 7.4. The GYP-loaded alginate beads in the gastric buffer (pH 1.2) were in a un-ionized state that brought a compact network structure with small pores because of the reducing electrostatic repulsion between the alginate molecules. As a result, the GYP diffusion was restricted and consequently the release fraction was relatively low. However, in the intestinal buffer (pH 7.4), the degree of ionization of the carboxyl groups along alginate chains increased, leading to an increase in the electrostatic repulsion and pore size. This allowed GYP to diffuse more efficiently and obtain the high release fraction. The pH-dependent release profiles of bioactive compounds or drugs from the alginate-based beads were also reported in several articles [48-50].

To illustrate the release kinetics and release mechanism of GYP from the alginate beads, zero-order, first-order, Higuchi and Rigter-Peppas models were applied to fit the release data, and the kinetic parameters obtained by fitting shown in Table 3. The Rigter-Pep-

**Table 3. Curve fitting results of the release models**

| pH | Squared correlation coefficient ($R^2$) | | | | Release exponent (n) |
|---|---|---|---|---|---|
| | Zero-order | First-order | Higuchi | Rigter-Peppas | |
| 1.2 | 0.9450 | 0.9787 | 0.9728 | 0.9939 | 0.7525 |
| 7.4 | 0.7622 | 0.9391 | 0.7027 | 0.9880 | 0.9482 |

**Table 4. Curve fitting results of Peppas-Sahlin equation (m=0.43)**

| pH | $k_1$ | $k_2$ | $k_2/k_1$ | $R^2$ |
|---|---|---|---|---|
| 1.2 | 0.01133 | 0.00659 | 0.58 | 0.99209 |
| 7.4 | 0.02626 | 0.03819 | 1.45 | 0.98933 |

pas model had the highest squared correlation coefficient ($R^2$) at both pH 1.2 ($R^2$=0.9939) and pH 7.4 ($R^2$=0.9880) by comparing those of the other three models, indicating the Rigter-Peppas model was the most proper model to evaluate the GYP release from the alginate beads. The release exponents (n) from the Rigter-Peppas model were 0.7525 (between 0.43 and 0.85) at pH 1.2 and 0.9482 (greater than 0.85) at pH 7.4. These results indicated the release mechanism of GYP at pH 1.2 was non-Fickian transport, controlled by the GYP diffusion and the swelling of the alginate beads [48]. In contrast, the release mechanism at pH 7.4 was case-II transport release, governed by the alginate matrix's swelling/relaxation [37]. The $k_1$ and $k_2$ values achieved from the Peppas-Sahlin equation by fitting the release data and the $k_2/k_1$ ratio are shown in Table 4. As seen in Table 4, the $k_2/k_1$ ratio at pH 1.2 and 7.4 was 0.58 and 1.45, respectively, indicating the GYP release at pH 1.2 was controlled by the diffusion, but at pH 7.4 was dominated by the matrix's swelling. A similar result was also found in the drug release from the ternary polymeric matrix [51].

The antioxidant activity of the unencapsulated and encapsulated GYP was measured by the DPPH method. The unencapsulated GYP and the released GYP from the alginate beads on the first day were 0.91 and 0.86 mg Vc/mg, respectively, but on the 15th day, they were 0.55 and 0.71 mg Vc/mg, respectively. As shown in the above test data, on the 15th day, the encapsulated GYP's antioxidant activity was 1.29 times that of the unencapsulated GYP, and it also retained 82.56% of the antioxidant activity compared with the first day. These indicated that the encapsulated GYP had effectively maintained its antioxidant activity and biological activity.

## CONCLUSIONS

The GYP-loaded alginate beads were fabricated by ionic gelation technique, and preparation parameters were optimized by RSM. The optimal conditions for the highest encapsulation efficiency were alginate concentration of 3.3%, $CaCl_2$ concentration of 2.4%, and GYP concentration of 3.2 mg/mL. The GYP-loaded alginate beads had a roughly spherical morphology with a wrinkled surface, and their average diameter was 0.87 mm. The release behavior of GYP from the alginate beads was most appropriately evaluated by the Rigter-Peppas model. The release mechanism of GYP was non-Fickian transport and case-II transport at pH 1.2 and 7.4, respectively. The encapsulated GYP had good retention of its antioxidant activity and biological activity. Polysaccharides and proteins used as filler ingredients can improve the alginate beads' wrinkled surface after lyophilization.

## ACKNOWLEDGEMENTS

This work was financially supported by the University Student Innovation and Entrepreneurship Training Program of Guangdong Province (No. 201610580058).

## REFERENCES

1. L. Chen, M. Li, Z. Yang, W. Tao, P. Wang, X. Tian, X. Li and W. Wang, *J. Ethnopharmacol.*, **257**, 112829 (2020).
2. K. Okoshi, Y. Uekusa, Y. Narukawa and F. Kiuchi, *J. Nat. Med.*, **75**, 76 (2021).
3. H. B. Li, J. F. Ma, Y. D. Mei, L. X. Liu, Z. Y. Cao, D. F. Shi, X. S. Yao and Y. Yu, *Nat. Prod. Res.* (2020), https://doi.org/10.1080/14786419.2020.1775227.
4. N. Zhang, M. Luo, L. He and L. Yao, *Molecules*, **25**, 4702 (2020).
5. Q. Chen, G. Xue, Q. Ni, Y. Wang, Q. Gao, Y. Zhang and G. Xu, *Food Sci. Nutr.*, **8**, 1 (2020).
6. J. Wu, J. Zhang, X. Yu, Y. Shu, S. Zhang and Y. Zhang, *Food Sci. Nutr.*, **9**, 822 (2021).
7. W. Xu, J. Yu, W. Feng and W. Su, *Molecules*, **21**, 540 (2016).
8. W. Xiao, S. Li, S. Wang and C. T. Ho, *J. Food Drug Anal.*, **25**, 43 (2017).
9. S. Jurić, M. Jurić, Ż. Król-Kilińska, K. Vlahoviček-Kahlina, M. Vinceković, V. Dragović-Uzelac and F. Donsì, *Food Rev. Int.* (2020), https://doi.org/10.1080/87559129.2020.1837862.
10. M. Utpott, R. Q. Assis, C. H. Pagno, S. P. Krigger, E. Rodrigues, A. d. O. Rios and S. H. Flôres, *Food Bioprocess Technol.*, **13**, 1940 (2020).
11. M. C. Otálora, J. G. Carriazo, L. Iturriaga, C. Osorio and M. A. Nazareno, *Food Chem.*, **202**, 373 (2016).
12. F. T. V. Rubio, C. W. I. Haminiuk, M. Martelli-Tosi, M. P. d. Silva, G. Y. F. Makimori and C. S. Favaro-Trindade, *Food Res. Int.*, **136**, 109470 (2020).
13. Y. Li, B. Tang, J. Chen and P. Lai, *Food Sci. Technol.*, **38**, 530 (2018).
14. R. Cortez, D. A. Luna-Vital, D. Margulis and E. G. d. Mejia, *Compr. Rev. Food Sci. Food Saf.*, **16**, 180 (2017).
15. S. C. Siang, L. K. Wai, N. K. Lin and P. L. Phing, *Food Sci. Technol.*, **39**, 601 (2019).
16. N. D. A. Arriola, P. I. Chater, M. Wilcox, L. Lucini, G. Rocchetti, M. Dalmina, J. P. Pearson and R. D. d. M. C. Amboni, *Food Chem.*, **275**, 123 (2019).
17. F. E. Vasile, M. A. Judis and M. F. Mazzobre, *Food Chem.*, **250**, 75 (2018).
18. M. C. Otálora, J. G. Carriazo, C. Osorio and M. A. Nazareno, *Food Res. Int.*, **111**, 423 (2018).
19. G. Liu, Z. Hu, R. Guan, Y. Zhao, H. Zhang and B. Zhang, *Korean J. Chem. Eng.*, **33**, 3141 (2016).
20. S. Cho, J. W. Kang and J. Lee, *Korean J. Chem. Eng.*, **37**, 1726 (2020).
21. J. Orozco-Villafuerte, A. Escobar-Rojas, L. Buendía-González, C. García-Morales, C. Hernandez-Jaimes and J. Alvarez-Ramirez, *J. Dispersion Sci. Technol.*, **40**, 1065 (2019).
22. T. C. B. Gallo, M. G. Cattelan, I. D. Alvim and V. R. Nicoletti, *J. Food Process. Preserv.*, **44**, e14947 (2020).
23. S. Gholamian, M. Nourani and N. Bakhshi, *Food Chem.*, **338**, 128143 (2021).
24. T. R. A. Calvo, M. Perullini and P. R. Santagapita, *J. Food Eng.*, **235**, 32 (2018).
25. I. Niizawa, B. Y. Espinaco, S. E. Zorrilla and G. A. Sihufe, *Int. J. Biol. Macromol.*, **121**, 601 (2019).

26. A. G. d. S. Carvalho, M. T. d. CostaMachado, H. D. d. F. Q. Barros, C. B. B. Cazarin, M. R. M. Junior and M. D. Hubinger, *Powder Technol.*, **345**, 283 (2019).
27. Y. Liu, C. Y. Li, H. M. Huang, H. H. Peng, M. Y. Shen and X. H. Hu, *Food Industry*, **38**, 84 (2017).
28. X. Zhu, Y. Mang, F. Shen, J. Xie and W. Su, *J. Food Sci. Technol.*, **51**, 1575 (2014).
29. Y. Liu, S. Wei and M. Liao, *Ind. Crop. Prod.*, **49**, 837 (2013).
30. L. Gu, D. J. McClements, J. Li, Y. Su, Y. Yang and J. Li, *Food Hydrocolloid.*, **112**, 106349 (2021).
31. N. A. Peppas and J. J. Sahlin, *Int. J. Pharmaceut.*, **57**, 169 (1989).
32. W. R. Gombotz and S. F. Wee, *Adv. Drug Delivery Rev.*, **64**, 194 (2012).
33. I. Rousseau, D. L. Cerf, L. Picton, J. F. Argillier and G. Muller, *Eur. Polym. J.*, **40**, 2709 (2004).
34. B. P. Hills, J. Godward, M. Debatty, L. Barras, C. P. Saturio and C. Ouwerx, *Magn. Reson. Chem.*, **38**, 719 (2000).
35. M. Bilal and H. M. N. Iqbal, *Biocatal. Agric. Biotechnol.*, **20**, 101205 (2019).
36. J. Zhang, H. H. Li, Y. F. Chen, L. H. Chen, H. G. Tang, F. B. Kong, Y. X. Yao, X. M. Liu, Q. Lan and X. F. Yu, *J. Zhejiang Univ. Sci. B*, **21**, 611 (2020).
37. K. Benfattoum, N. Haddadine, N. Bouslah, A. Benaboura, P. Maincent, R. Barillé, A. Sapin-Minet and M. S. El-Shall, *Polym. Adv. Technol.*, **29**, 884 (2018).
38. G. B. Celli, A. Ghanem and M. S. L. Brooks, *J. Berry Res.*, **6**, 1 (2016).
39. Z. Jiang, Y. Zhang, J. Li, W. Jiang, D. Yang and H. Wu, *Ind. Eng. Chem. Res.*, **46**, 1883 (2007).
40. Q. B. Tu, P. Y. Wang, S. Sheng, Y. Xu, J. Z. Wang, S. You, A. H. Zhu, J. Wang and F. A. Wu, *Waste Biomass Valor.*, **11**, 5273 (2020).
41. M. Chen, Y. Hu, J. Zhou, Y. Xie, H. Wu, T. Yuan and Z. Yang, *RSC Adv.*, **16**, 13032 (2016).
42. Y. Liu, S. Wei, L. Liu, M. Liao and Y. Huang, *RSC Adv.*, **5**, 5533 (2015).
43. M. Zhou, Q. Hu, T. Wang, J. Xue and Y. Luo, *Int. J. Biol. Macromol.*, **120**, 859 (2018).
44. Q. Li, M. Duan, D. Hou, X. Chen, J. Shi and W. Zhou, *Food Hydrocolloid.*, **112**, 106274 (2021).
45. A. Bušić, A. Belščak-Cvitanović, A. V. Cebina, S. Karlović, V. Kovač, I. Špoljarić, G. Mršić and D. Komes, *Food Res. Int.*, **111**, 244 (2018).
46. A. Belščak-Cvitanović, D. Komesa, S. Karlović, S. Djaković, I. Špoljarić, G. Mršić and D. Ježek, *Food Chem.*, **167**, 378 (2015).
47. K. Essifi, M. Lakrat, D. Berraaouan, M. L. Fauconnier, A. E. Bachiri and A. Tahani, *Polym. Bull.* (2020), https://doi.org/10.1007/s00289-020-03397-9.
48. O. J. Olayemi, Y. E. Apeji and C. Y. Isimi, *J. Pharm. Innov.* (2020), https://doi.org/10.1007/s12247-020-09509-2.
49. Z. C. Yin, Y. L. Wang and K. Wang, *J. Drug Deliv. Sci. Technol.*, **43**, 12 (2018).
50. X. Sun, C. Liu, A. M. Omer, L. Y. Yang and X. K. Ouyang, *Int. J. Biol. Macromol.*, **132**, 487 (2019).
51. H. Kim and R. Fassihi, *Pharm. Res.*, **14**, 1415 (1997).